This manuscript was published as formal in:

Polymer Chemistry 2018, 9, 2359-2369

DOI: 10.1039/c7py01678f

https://doi.org/10.1039/C7PY01678F

***Title*:**

Chitosan Hydrogelation with a Phenothiazine based Aldehyde – a Synthetic Approach toward Highly Luminescent Biomaterials

Andrei Bejan[1], Daniela Ailincai[1], Bogdan C. Simionescu[1,2], Luminita Marin[1]*

[1] *"Petru Poni" Institute of Macromolecular Chemistry, Romanian Academy, 700487 Iasi, Romania*

[2] *Department of Synthetic and Natural Polymers, "Gh. Asachi" Technical University of Iasi, 700050 Iasi, Romania*

*email: lmarin@icmpp.ro

Abstract

Pure organic luminescent hydrogels were synthesised using condensation reaction of amino groups of chitosan with a photoactive aldehyde bearing phenothiazine moiety. The hydrogels were structurally and supramolecularly characterized by FTIR and ^{1}H-NMR spectroscopy, X-ray diffraction and polarized light microscopy. It was concluded that hydrogelation occurred due to the self-ordering of the chitosan segments grafted with pendant phenothiazine imines into ordered clusters, which play the role of crosslinking nodes. Scanning electron microscopy revealed microporous morphology with very thin pore walls. The ordered clusters immobilized in the polycationic chitosan network were responsible for high quantum efficiency, reaching the value of 51% in the xerogel state. The hydrogels formed flexible, transparent films with high mechanical toughness. Beside the remarkable optical and mechanical properties, the importance of the hydrogels is increased by their eco-design, based on chitosan from renewable resources and bio-friendly phenothiazine.

Keywords: chitosan, phenothiazine, hydrogels, luminescence, renewable resources

Introduction

Organic materials for opto-electronic applications have been intensely studied in the last decades as a cheaper and more environmentally friendly alternative to inorganic ones [1]. The real world applications require highly efficient luminescent materials in solid state, a desideratum difficult to attain for organic luminogens which present the tendency to aggregation-caused quenching [2]. Among organic luminescent materials, the concept of luminescent hydrogels has received increasing attention in the last years, due to their unique physico-chemical characteristics which render them proper in special biomedical applications, such as bioimaging agents, tissue engineering, molecular thermometers, 3D-printing [3-5], but also in classic photonics, as organic light emitting diodes, solar cells or fluorescent sensors [6-10]. Their high content of water endows them with good transparency and mouldability, while their three-dimensional network confers them good mechanical properties [11,12]. Besides, the high surface-to-volume ratio of the micro- or nano-porous hydrogels is a promising feature to improve the optical properties [13], making them more attractive for integration in modern device architectures. Remarkable endeavour has been directed towards obtaining of luminescent organic-inorganic hybrid hydrogels, mainly using lanthanide complexes as photoactive components, due to their phosphorescence properties [14]. The best results reported a quantum yield up to 70 %, but the stability of their efficiency is significantly affected by the non-radiative decay in aqueous environments [15, 16]. By contrast, luminescent hydrogels

obtained using organic dyes are less reported, and their quantum efficiency is rather modest [15-18]. The main difficulty in obtaining pure organic hydrogels is the low water solubility of the organic dyes, while their specific emission quenching and photobleaching discouraged research in this direction. The two important advantages of luminescent hydrogels based on biopolymers from renewable resources are their potential for bio-application, due to their biocompatibility and biodegradability, and their sustainable development, which enhances even more their practical value [19]. In this regard, the latest research in the field of luminescent hydrogels has been focused on the use of bio-based materials, such as cellulose [20-22], phtalocyanines, porphyrins [23] or amino acids [24] as matrix for photoactive compounds as lanthanides, quantum dots or organic dyes. Nevertheless, the quantum yield was still low for their use in photonics, the obtained materials being especially studied for sensing applications [25-28].

Chitosan is a biopolymer originating from chitin, the second most abundant natural polymer [29]. Our research activity in the field of chitosan derivatives revealed a new concept of chitosan hydrogelation when reacting with monoaldehydes [30-35], experimentally signalled by other authors too [36]. The driving force of this unusual hydrogelation has been demonstrated to consist in the ability of the chitosan segments grafted with imine units to self-order in clusters, which act as network nodes. The new method proved to be a practical strategy towards advanced biomaterials, due to the large variety of monoaldehydes, many of them coming from natural resources, which allow the tailoring of hydrogel properties. Applying this simple principle, supramolecular hydrogels with *in vivo* biocompatibility and outstanding antifungal, swelling or antitumor properties were successfully obtained [32-35]. The main issue of the method is to find proper reaction conditions for the organic aldehyde with chitosan in aqueous solution.

In this paper we report new pure organic hydrogels obtained by acid condensation of a photoactive monoaldehyde with chitosan polyamine. A phenothiazine bearing monoaldehyde has been chosen as fluorogen [37], since imines-based phenothiazine heteroaromatic ring proved high quantum efficiency in solid state [38-40]. Moreover, films obtained from chitosan and phenothiazine showed green light emission [41]. As a proof of concept, the synthesised hydrogels proved high quantum efficiency in both hydrogel and xerogel state and excellent mechanical properties.

Experimental

Materials

Low molecular weight chitosan (263 kDa) with a degree of deacetylation (DA) of 83 %, acetone (99 %), dimethylsulfoxide (UV-spectroscopy 99.8 %) and glacial acetic acid (98 %) were purchased from Sigma–Aldrich Co (USA) and used as received. The ethylic alcohol (96 %) from Sigma–Aldrich was dried on molecular sieves before use. The molecular sieves (2 Å) from Sigma–Aldrich were dried before use, at 80 ^{o}C under vacuum for three days. The luminescent aldehyde has been synthesised in our laboratory following a published procedure [37]. Its solubility in ethanol was 2 mg/mL. Its structure and structural characterization are given below.

10-(-4-Hexyloxy-phenyl)-10H-phenothiazine-3-carbaldehyde (**FhA**), m.p. = 108 – 109.8 ^{o}C

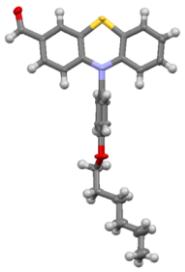

^{1}H NMR (400.13 MHz, DMSO-d_6, ppm) δ = 9.76 (s, 1H), 7.50 (s, 1H), 7.44 (d, 1H), 7.38 (d, 2H), 7.26 (d, 2H), 7.04 (d, 1H), 6.97-6.89 (superposed bands, 2H), 6.30 (d, 1H), 6.22 (d, 1H), 4.14 (t, 2H), 1.90-1.83 (m, 2H), 1.59-1.39 (superposed bands, 6H), 0.94 (t, 3H); FT-IR (KBr, cm^{-1}): 3059, 3021 ($\nu_{CHaromatic}$), 2945, 2920, 2855 (ν_{CH3}, ν_{CH2}), 1675 ($\nu_{C=O}$), 1595, 1504 ($\nu_{C=Caromatic}$), 1239 (ν_{C-O-C}), 836, 813, 744 ($\delta_{CHaromatic}$); X-ray crystallography: $C_{25}H_{25}NO_2S$, T=175 K, Mr=403.5 gmol^{-1}; space group $P2_1/c$; cell lengths: a=13.6446(5), b=14.2470(5), c=10.9711(4); cel angles: α=90.00^{o}, β=94.954(3)^{o}, γ=90.00^{o}; cell volume: V=2124.76 Å^3; Z=4, R=5.06 %.

Preparation of hydrogels and xerogels

In a 20 mL vial, a chitosan solution has been prepared from 30 mg chitosan (0.147 mmols of glucosamine repeating units) dissolved in 1.5 mL solution of acetic acid 0.7 % (10.5 µL glacial acetic acid in 1.489 mL bidistilled water), at room temperature. To obtain hydrogels with different content of luminogen, a solution of aldehyde (**FhA**) has been prepared by dissolving various amounts of **FhA** in 340 µL DMSO (Table 1). Both solutions were heated at 65 ^{o}C and the aldehyde one has been slowly dropped into the chitosan one under vigorous magnetic stirring. A viscous solution, opaque yellow in colour, has been obtained through the process. Further, 1 mL of acetone was slowly dropped into the reaction mixture, resulting in a transparent semisolid, which passed the inversion test used for visual assessing of the hydrogels

(Scheme 1). The hydrogels were kept uncovered for three days at room temperature to let the acetone evaporate. To remove the DMSO and the traces of unreacted aldehyde, the hydrogels were washed by successive immersions of 30 minutes each in portions of 20 mL dry ethanol, until the alcohol remained colourless, without light emission when illuminated with an UV lamp, and hydrogels were macroscopically homogeneous, with no visible aggregates inside. Further, in order to rehydrate the hydrogels and to remove the ethanol, they were immersed five successive times in portions of 20 mL water. The hydrogel synthesis has been performed in triplicate, starting from three different amounts of chitosan: 30, 60 and 90 mg, respectively, for all five different molar ratios. In all cases, the hydrogelation successfully occurred. The corresponding xerogels were prepared by lyophilization.

Table 1. Reagent and product amounts used in hydrogels obtaining and their codes

Code	**CPA1**	**CPA2**	**CPA3**	**CPA4**	**CPA5**
NH_2/CHO molar ratio[1]	1:0.05	1:0.1	1:0.2	1:0.3	1:0.4
Chitosan (g)	0.03	0.03	0.03	0.03	0.03
Aldehyde (g)	0.00295	0.0059	0.0118	0.0178	0.02375
Xerogel (g)	0.03241	0.0348	0.0412	0.0475	0.04969
η% (C<u>H</u>O→C<u>H</u>=N)[2]	82	81	94	98	83
η% (NH_2→CH=N)[3]	4.1	8.1	18.8	29.4	33.2

[1] calculated with eq.1 given in ESI; [2] calculated with eq.2 given in ESI; [3] calculated with eq.3 given in ESI

Methods

The corresponding xerogels were obtained by freezing the rehydrated hydrogels in liquid nitrogen and further lyophilization using LABCONCO FreeZone Freeze Dry System equipment, at -50 ºC and 1.510 mbar for 24 hours.

FTIR spectra were recorded on xerogel samples, using a FTIR Bruker Vertex 70 Spectrometer, by ATR technique, at room temperature, with a resolution of 2 cm^{-1} and accumulation of 32 scans. They were processed using Opus6.5 and Origin8 software.

^{1}H-NMR spectra were recorded on Bruker Avance DRX 400 MHz Spectrometer equipped with a 5 mm QNP direct detection probe and z-gradients, at room temperature, with an accumulation of 64 scans. The chemical shifts were reported as δ values (ppm) relative to the residual peak of the solvent. The hydrogel sample has been prepared into the NMR tube using deuterated solvents (D_2O to solve chitosan, DMSO-d6 to solve the aldehyde, and $(CD_3)_2CO$ for hydrogelation). The sample preparation succeeded only in the case of the **CPA1** hydrogel. For

the others, in the absence of a vigorous stirring impossible to be provided into the NMR tube, the aldehyde abundantly crystallized hindering hydrogelation.

Wide angle X-ray diffraction (WXRD) was performed on xerogel pellets using a Bruker D8 Avance diffractometer with Ni-filtered Cu-Ka radiation of l = 0.1541 nm, in the range of 2-40° (2 theta). The working conditions were 36 kV and 30 mA. Data were handled by the FullProf 2000 program. The xerogel pellets were obtained with a manual Hydraulic Press, by applying a pressure of 10 N m^{-1}.

Textures of the hydrogels were monitored on thin slices of samples placed between two clean glass slides with an Olympus BH-2 polarized light microscope equipped with a THMS 600 heating stage and a LINKAM TP92 temperature control system.

Micrometric images of the xerogels were acquired with a Scanning Electron Microscope SEM EDAX – Quanta 200 at accelerated electron energy of 20 KeV.

The UV-Vis absorption spectra were registered with a Carl Zeiss Jena Specord M42 instrument, by using very thin hydrogel films deposited on glass plates.

The absolute values of the quantum yield (Φ_{fl}) of the hydrogels and xerogels, respectively, were obtained with a FluoroMax-4 spectrofluorometer equipped with a Quanta-phi integrating sphere accessory Horiba Jobin Yvon, by exciting the samples with light of wavelength corresponding to the absorption maxima from UV-vis spectra, at room temperature. To obtain a good optical luminescence signal-to-noise ratio, the slit widths and detector parameters were optimized to maximize but not saturate the excitation Rayleigh peak. The measurements were carried out in triplicate for each sample. Close values were obtained.

Tensile strength of the hydrogels was recorded for a rectangular piece (20x5x0.5 mm^3) of six different samples on TIRA test 2061 equipment Maschimnbau GmbH Ravenstein, Germany. Measurements were done on triplicate samples, at an extension rate of 50 mm x min^{-1}, at room temperature and the average value was reported. Elongation tests were performed by applying an elongation of 20, 40, 50, 60, 80 and 100 %. The sample has been kept elongated for 20 minutes, and then allowed to relax for 5 minutes. The viscoelastic loss was calculated as the difference between the initial length and the length after applying the elongation test.

Results and discussion

Hydrogelation mechanism. Experimental evidence

Luminescent hydrogels were prepared by grafting phenothiazine-bearing aldehydes on chitosan backbone *via* acid condensation reaction, when imine linkages were formed (Scheme 1). DMSO – a biodispersant with high solvation power – was used as solvent of the aldehyde,

to avoid its crystallization in aqueous medium of chitosan solution. Acetone has been used as co-solvent to ensure a homogeneous reaction medium. Varying the molar ratio of the aldehyde and amine functionalities, a series of hydrogels with different content of imino-phenothiazine photoactive units was obtained. The minimum amount of aldehyde necessary for chitosan gelling corresponded to NH_2/CHO = 1/0.05 (**CPA1**). The maximum amount of aldehyde used for chitosan gelling without its abundant crystallization corresponded to NH_2/CHO = 1/0.4 (**CPA5**). Hydrogels formation was firstly assessed by visual inspection using the inversion test (Scheme 1). Under illumination with an UV-lamp, they strongly emitted green light, indicating that the photoactivity of the phenothiazine was kept by gelling.

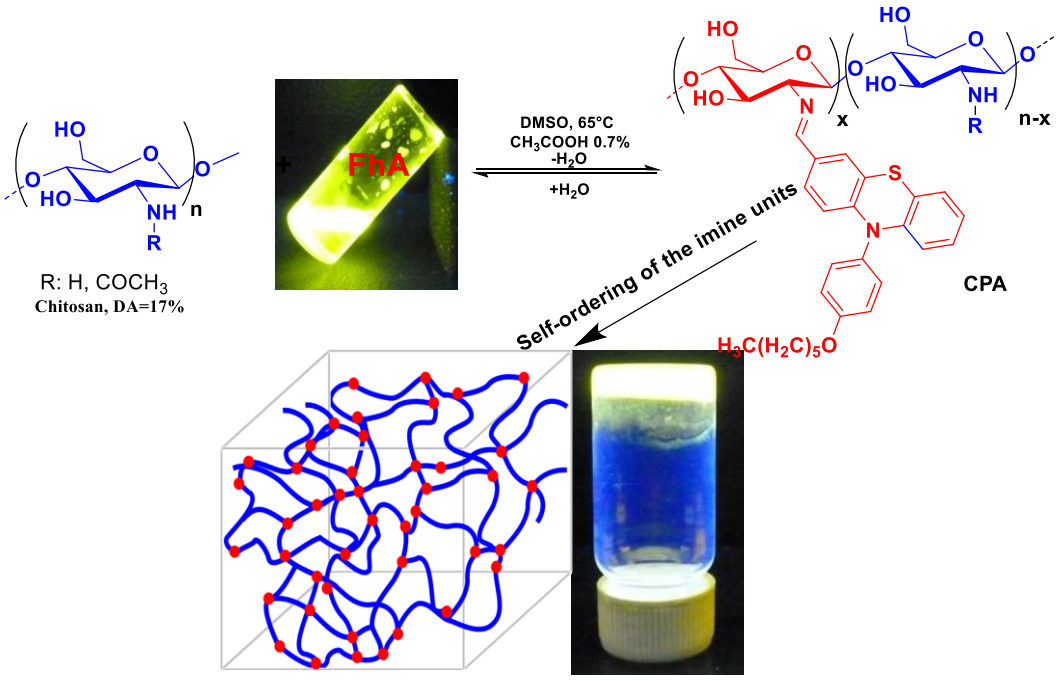

Scheme 1. Schematic representation of the synthesis of the luminescent hydrogels

The successful grafting of the aldehyde on chitosan chains by imine linkage was demonstrated by FTIR spectra of the corresponding xerogels, which showed a vibration band at 1648 cm^{-1} as a slightly sharper peak as compared to the shoulder at 1639 cm^{-1} specific to the vibration band of the amide group of chitosan (Figure 1) [30-35, 42]. Taking into consideration that vibration band of the aliphatic-aromatic imine bond is shifted to higher wavenumbers compared to aromatic-aromatic ones, this was attributed to the newly formed imine bonds [31]. No evident aldehyde band was observed around 1675 cm^{-1} [37], indicating the preponderance of the photoactive phenothiazine as imine units. Comparing the FTIR spectra of the **CPA1** – **CPA5** xerogels with that of chitosan, changes were obvious in the 3700 – 2700 cm^{-1} region, which is characteristic to the asymmetric and symmetric N-H stretch and vibrations of the intra-

and inter-molecular hydrogen bonds [30]. The change involved the shifting of the overlapped bands to higher wavenumbers, suggesting morphological modifications, in agreement with the grafting of the rigid imine units on the semiflexible chitosan chains [30-35]. Moreover, changes occurred in the intensity of the band maxima attributed to the stretching vibration of the C-O bond (1069 and 1031 cm $^{-1}$) [33]. As can be seen in figure 1, the maximum at 1031 cm^{-1} increased in intensity and the maximum at 1069 cm^{-1} decreased for the **CPA1**-**CPA5** samples compared to that of chitosan. Considering that this band is strongly influenced by the H-bonds environment, the change was also attributed to the morphological rearrangements due to the imination.

The successful grafting of the phenothiazine moieties onto chitosan chains by imine linkages was further proved by the ^{1}H-NMR spectrum recorded on the **CPA1** freshly prepared hydrogel, before washing. It revealed the chemical shift of the imine proton at 8.5 ppm as two bands corresponding to α and β conformers (Figure 1s) [33, 43]. The chemical shift of the aldehyde proton was also present in the NMR spectrum, with an integral ratio of C<u>H</u>O/C<u>H</u>=N of 1/3.7. This indicated the shifting of the reaction equilibrium to the imino-chitosan product (a glycodynamer due to the reversible imine linkages) with a conversion rate of the aldehyde into imine units of 79 %. This means that in the case of **CPA1**, about 4 % from the amine groups on chitosan were transformed in imine linkages. The estimation of the conversion rate from ^{1}H-NMR spectrum agrees well with the calculation from the weighting measurements (see Experimental section), displaying an average conversion of the aldehyde into imine units at around 90 %, i.e. the percent of the amine units converted into imine ones on the chitosan chains varied from 4.2 to 33.2 % (Table 1). The shifting of the reaction equilibrium to the imine products was attributed to the formation of the phenothiazine-imine donor-acceptor system with high stability [38, 39].

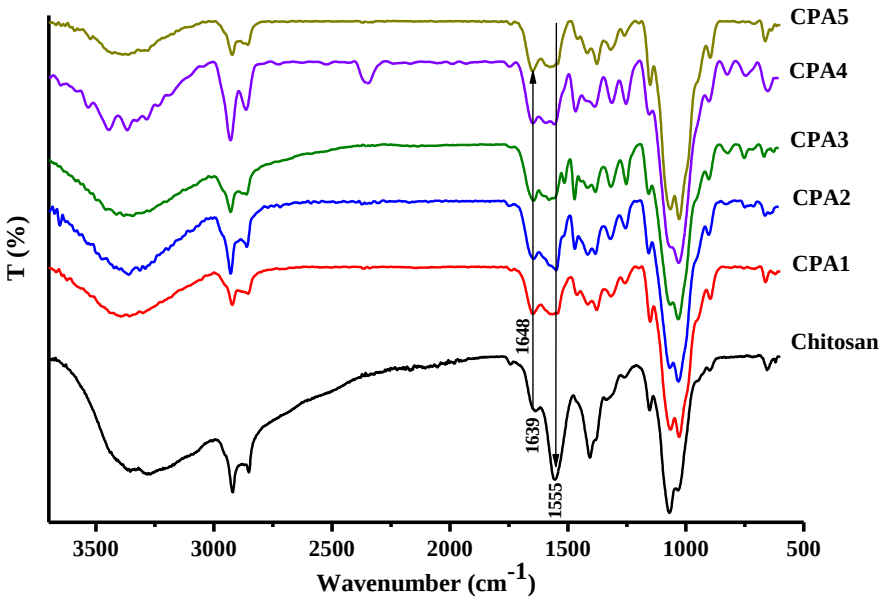

Figure 1. FTIR spectra of **CPA1** – **CPA5** xerogels and chitosan

To have an insight on the morphological changes suggested by FTIR spectroscopy, X-ray diffraction has been performed on xerogels pellets. As can be seen in Figure 2, the semicrystalline chitosan transformed by imination into a more ordered material, characterised by a sharp reflection in the medium angle domain, at 6.4 º, sharper reflection peaks on the top of the broad reflection in the wide angle region, around 20 º and a sharp band at 29.4 º, and a slight broad band around 12 º. The corresponding d-spacing, as calculated using Bragg low was around 13.8, 4.4, 3.15, and 7.4 Å, respectively. Compared to other phenothiazine imine derivatives, the position of the reflection bands is quite similar, this signifying a similar ordering pattern. As an example, an imine bearing phenothiazine residue showed in single crystal X-ray diffraction a packing of the molecules in ribbons with intermolecular distance of 8.2 Å, further packed in layers with inter-ribbons distance of 3.8 Å and inter-layer distance of 15.3 Å [38, 44]. By similarity it can be foreseen a layered packing of the chitosan segments grafted with phenothiazine imine units. Compared to other imino-chitosan derivatives [30-35, 45], the sharper peaks at lower angle were of lower intensity or even missing, in agreement with the low amount of imine units on the chitosan backbones. However, the diffraction pattern was quite similar in the case of **CPA2**, **CPA3**, **CPA4** samples, with sharper reflection bands around 6 and 20 º and a broad reflection around 12 º – attributed to the inter-layer, inter-chain and inter-molecular distances of a supramolecular layered architecture resulted due to (i) the

hydrophobic/hydrophilic segregation of the hydrophobic imine units and hydrophilic chitosan chains, and (ii) self-ordering of the hydrophobic imines. The hydrogelation can be explained considering that the same chitosan chain can pass through different ordered clusters, thus forming a network in which the ordered clusters play the role of crosslinking nodes, as represented in Scheme 1. The lower density of imine units (**CPA1**) led to a relatively lower amount of crosslinking nodes as compared to the higher amount of chitosan, below the detection limit of the diffractometer. On the other hand, the formation of smaller ordered clusters in the case of **CPA5** sample, with weak positional order and long-range directional order, also led to the absence of specific reflections in the X-ray diffraction. The broad reflection of the chitosan X-ray pattern became slightly broader into those of the xerogels, in agreement with the linking of the chitosan chains between the ordered clusters, fact which hinder their H-bonding leading to a more disordered chitosan phase. In the light of these data, the chitosan crosslinking appears to be the result of the self-ordering process of the chitosan segments grafted with imine units, which represents the driving force of hydrogelation.

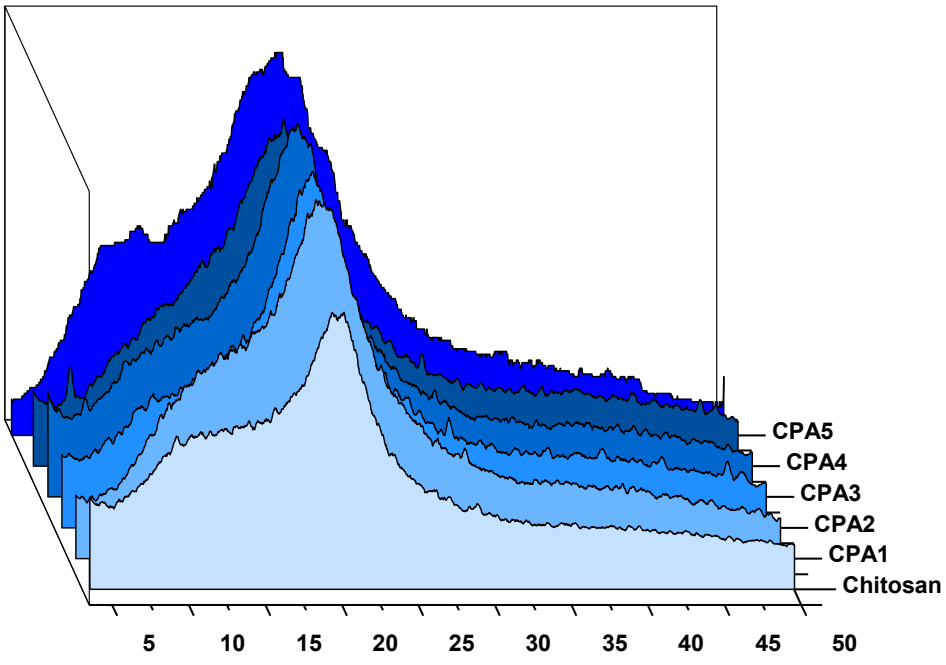

Figure 2. X-ray diffraction of chitosan and **CPA1** – **CPA5** xerogels

Thermotropic behavior

To further confirm the forming of the ordered clusters, the hydrogel samples were investigated by polarized light microscopy (POM). As can be seen in figure 3, all samples showed strong birefringence, typical for ordered systems, confirming the X-ray data. In the case of hydrogels containing lower amounts of phenothiazine units (**CPA1**, **CPA2**), rare, birefringent, rhomboedric geometric shapes could be detected, in line with the weak reflection at small angle in the X-ray pattern. As the amount of phenothiazine units increased, the geometric shapes decreased in size and became denser, giving a continuous optical texture in the case of **CPA5**, due to the superposing of the birefringent shapes across the sample [46, 47]. By heating the hydrogels, the birefringent shapes melted in isotropic state at temperatures around 75 ^{o}C in the case of the hydrogels with lower density of imine units (**CPA1**, **CPA2**, **CPA3**) and transformed into a Schlieren-like texture specific to the nematic mesophases in the case of the hydrogels with higher density of imine units (**CPA4**, **CPA5**) [48]. The stability range of the texture exceeded the temperature of thermal decomposition of chitosan [49]. The melting point was lower as compared to the one of the aldehyde precursor (108 – 109.8 ^{o}C). This suggests a less stiff supramolecular architecture of the ordered clusters, which can be attributed to the low mobility of the phenothiazine imine units on the semiflexible chitosan chains, hindering their close packing. Representative POM images were given in Figure 3.

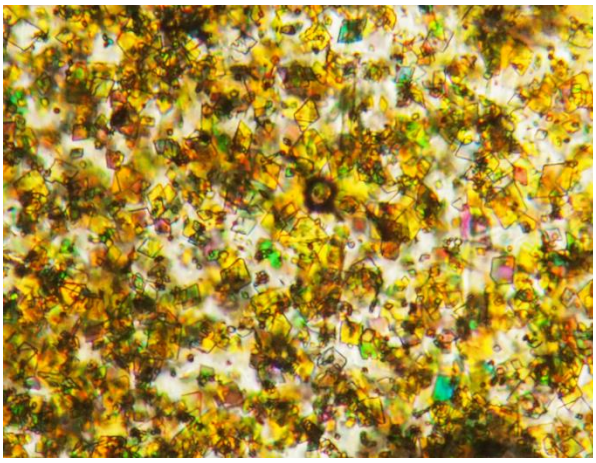

CPA1

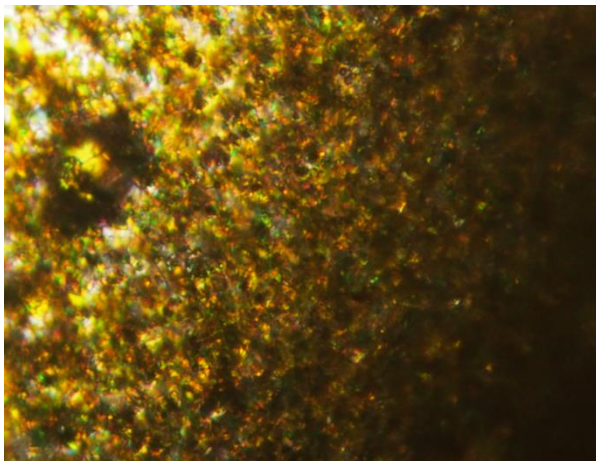

CPA2

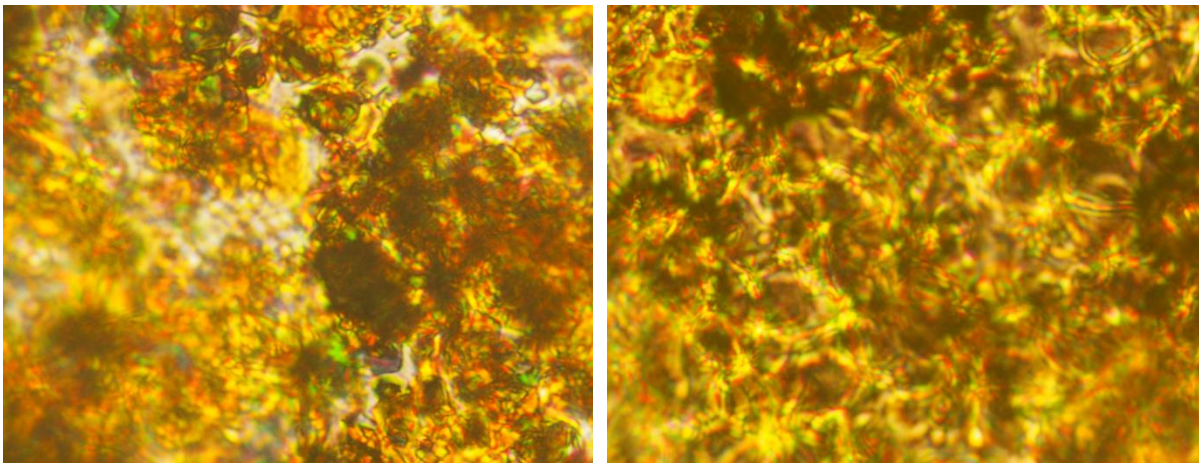

CPA4 **CPA4, 1C, 100 ºC**

Figure 3. Representative POM images of the hydrogels acquired, at 400x magnification (RT: room temperature, C: cooling)

Combining X-ray diffraction and polarized light microscopy data, the supramolecular architecture of the hydrogels could be envisioned as follows. When the concentration of the phenothiazine aldehyde was lower (**CPA1**, **CPA2**), the chitosan segments grafted with imine units segregated to form big, rare, layered clusters, similar to crystallization from diluted solutions. Their formation is favored by the carbonyl-amine/imine interconversion on the chitosan polyamine, acting as a molecular truck [50, 51]. Due to their smaller amount as compared to the larger amount of chitosan (aprox. 0.8/10; 1.28/10, weight ratio), their characteristic reflections couldn't be detected through the X-ray diffraction experiment. With increasing the amount of phenothiazine aldehyde (CPA3, CPA4), smaller crystals are formed due to the higher density of imine units and of such density that their sharper reflections in the X-ray diffractograms prevailed over the broad bands specific to the chitosan. At the highest amount of aldehyde (**CPA5**), denser and smaller crystals were formed, with weak positional order and long-range directional order, undetectable under X-ray diffraction [52-54]. Thus, the driving force of hydrogelation appears to be the formation of ordered clusters of variable size, anchored in the chitosan network. The size of the crystals decreases with increasing phenothiazine aldehyde amount, from **CPA1** to **CPA5**.

Microstructure

The hydrogel morphology at micrometric level, monitored by scanning electron microscopy of their corresponding xerogels, revealed a sponge like morphology with interconnected pores of diameter around 50 μm (Figure 4, Figure 2s). The remarkable part is

the extreme thinness of pore walls, attributed to the low density of the crosslinking nodes, leading to an elastic, hydrophilic network, able to hold large amounts of water and thus to form large pores during lyophilization process. No crystals were observed into the pores, this indicating that the crystals evidenced by XRD and POM measurements were placed into the solid walls of the pores.

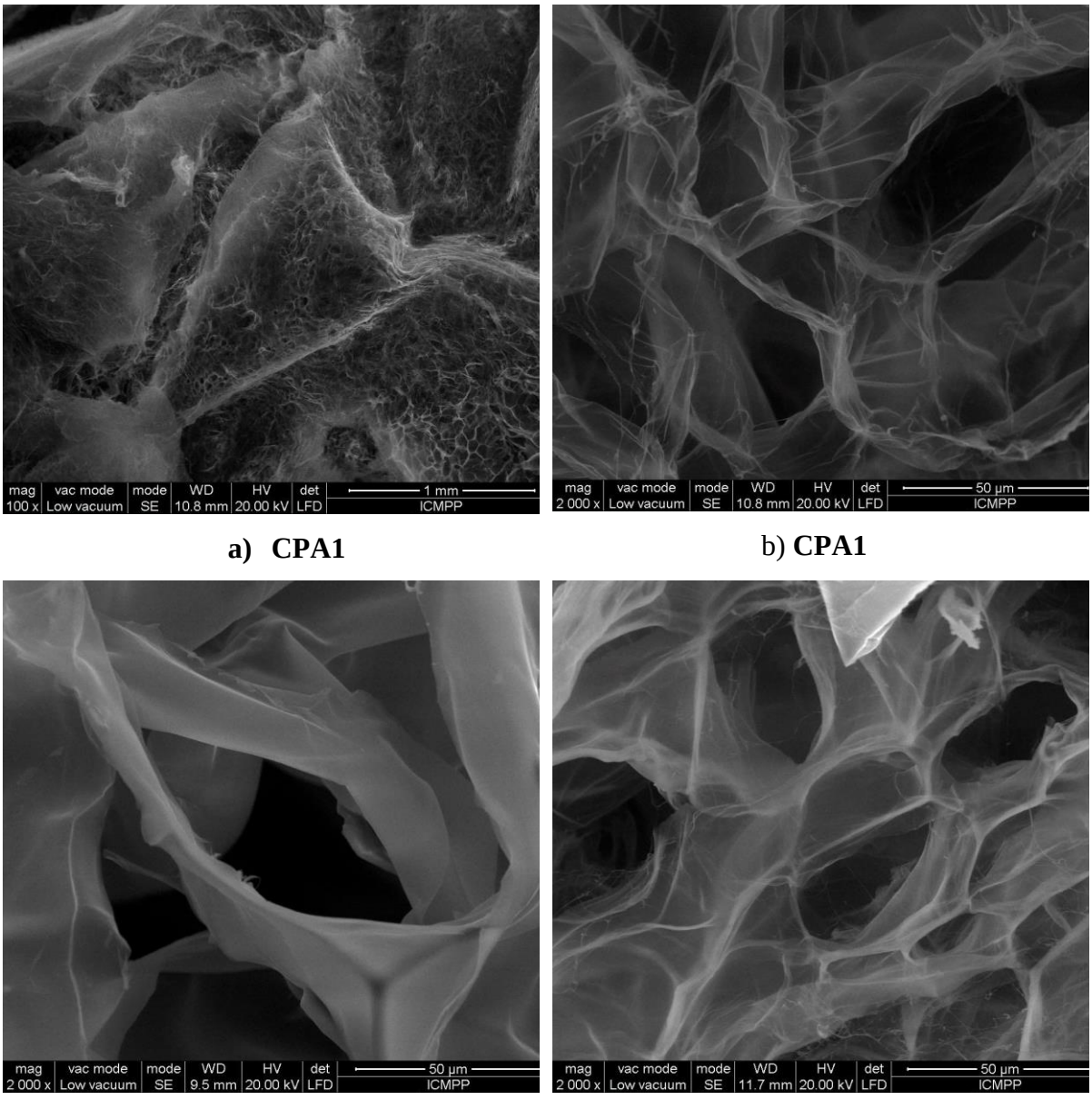

a) CPA1 b) **CPA1**

c) **CPA4** d) **CPA5**

Figure 4. SEM images of the hydrogels

Photophysical behavior of the hydrogels/xerogels

The chitosan-based hydrogels crosslinked with phenothiazine aldehyde were designed as luminescent materials for optoelectronics and sensing applications. It was expected that combining the high surface-to-volume ratio (characteristic to microporous materials) with the

emission ability of the phenothiazine fluorophore would result in efficient luminescent materials.

In this regard, the photophysical properties of both the hydrogels and the corresponding xerogels were monitored by absorption/emission spectroscopy, measuring the absorption and emission maxima, the Stokes shift, the quantum yield and the chromaticity coordinates. Besides, to better understand the origin of the photophysical properties, comparison with the aldehyde precursor and other imines bearing phenothiazine fluorophore were done.

The absorption spectra of the hydrogels exhibit overlapped bands with two maxima in the UV domain, around 360 and 395 nm, and a maximum of lower energy in the visible domain, around 480 nm, giving a broad absorption profile (Figure 5a), reminiscent of the absorption spectra of inorganic [55] or organic nanocrystals [40, 56-58]. Compared to the absorption spectrum of the aldehyde precursor [37] and other phenothiazine-imine derivatives [38, 39, 59], the electronic absorption maxima appear highly bathocromic shifted by around 80 nm. This is a characteristic behavior for organic aggregates stabilized in emulsions [60], similar to the studied hydrogels in which phenothiazine-based clusters are immobilized in the polycationic chitosan network (Figure 5b). (i) The absorption maximum around 360 nm has been attributed to the π-π* benzenoid transitions of the local aromatic units, (ii) the maximum around 395 nm to the electronic transition of the conjugated skeleton and (iii) the maximum around 480 nm to the D→A intramolecular charge transfer [38, 37, 61]. There is a close correlation between the supramolecular architecture of the hydrogels and the position of the absorption peaks that are almost 10 nm bathocromically shifted, as the size of the ordered clusters network nodes increases. This effect, well documented in literature, was attributed to the enhanced intermolecular forces as the cluster size increases [56, 57].

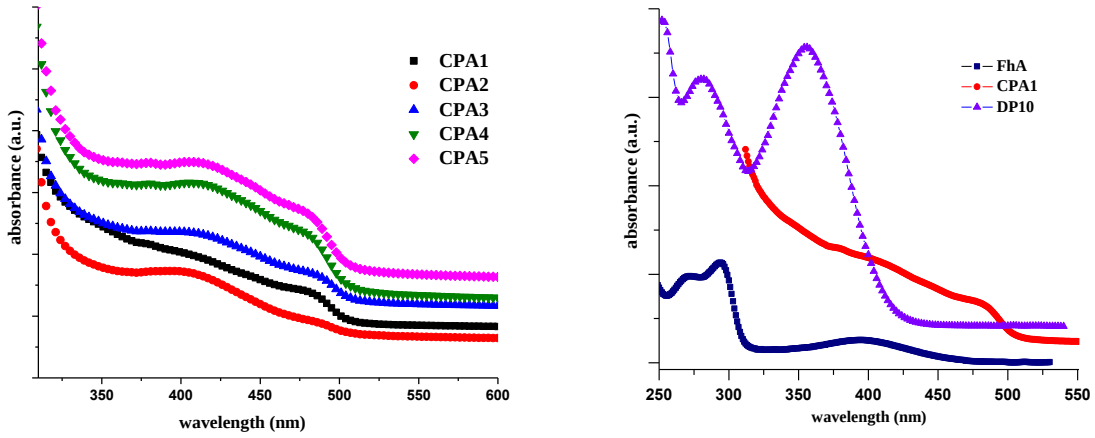

a) b)

Figure 5. UV-vis absorption of the (a) hydrogels and b) hydrogel **CPA1** compared to the THF solution of the **FhA** aldehyde precursor [37] and an phenothiazine-imine model compound (**DP10**) [38]

All hydrogels are transparent and formed flexible self-standing films when casted on a support (Figure 6g, h). Under UV illumination, they emitted strong green-yellow light (Figure 6i, j). Their photoluminescence properties were investigated by measuring the quantum yield and chromaticity diagrams when exciting the samples with the light of wavelength corresponding to the absorption maxima.

All hydrogels emitted light in the green domain, with an emission maximum red shifted from 522 to 532 nm as the wavelength of the exciting light increased from 360 to 480 nm (Figure 6a, b, c). When excited with higher wavelength light, the emission maxima slightly red shifted with increasing the size of the ordered clusters, effect considered to result from the diminishing of the Stokes shift (Table 1s) due to the configuration reorganization induced by the larger intermolecular interactions [58].

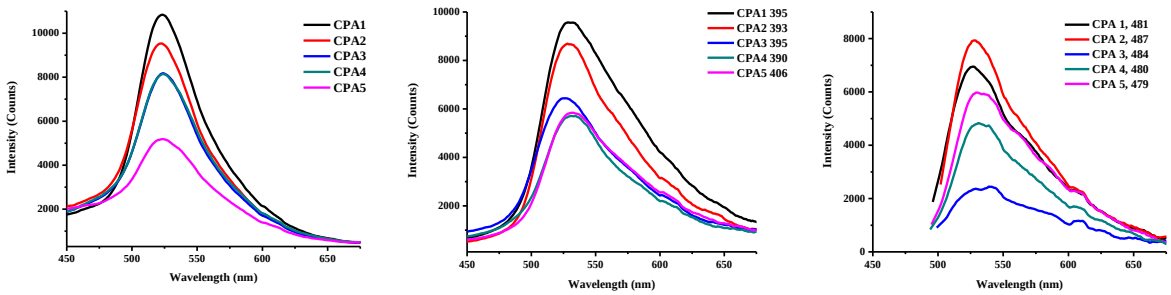

a) b) c)

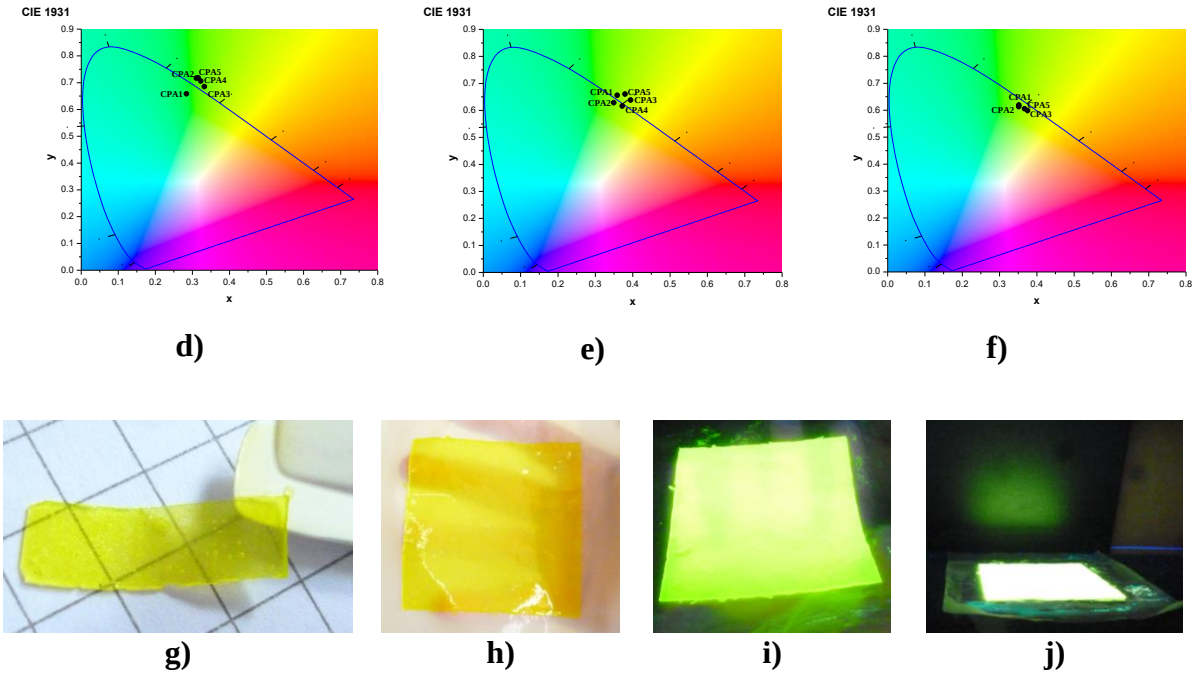

Figure 6. Emission spectra and chromaticity diagrams of the hydrogels when excited with light of a), d) 360 nm; b), e) around 395 nm and c), f) around 480 nm (the exact wavelength is given in the inset of the graph) and images of the **CPA1** hydrogel g, h) under normal light and i, j) when illuminated with an UV lamp

The quantum yield has high values, from 24.1 to 32.8 % (Table 2). When excited with higher energy light (UV light of 360 or 390-406 nm) only the **CPA1** and, **CPA1** and **CPA2**, respectively, emitted light in the gamut of human vision (Figure 6d, e). Decreasing the energy of the exciting light (green light of 479 – 487 nm) all the samples emitted pure light in the gamut of human vision close to the spectral locus (Figure 6f).

The quantum yield of the films obtained by air drying of the hydrogels gave similar results, while the chromaticity diagrams exhibited similar color of the emitted light.

Table 2. Values of the absolute quantum yield (Φ_{fl}) of the hydrogels and xerogels, excited with the absorption maxima

Code	Hydrogels			Xerogels		
	λex^1	λex^2	λex^3	λex^1	λex^2	λex^3
CPA1	25.4	29.1	32.8	43	25.7	11.4
CPA2	25.9	27.0	25.0	48.1	26.8	13.3
CPA3	29.3	25.2	26	40.4	24.7	14.3
CPA4	29.5	27	24.11	44.5	21.2	11.9
CPA5	29.8	25.3	32.1	51	25.8	9.8

λex^1: 360 nm; λex^2: 395; 393; 395; 390; 406; λex^3: 481; 487; 484; 480; 479

Xerogels exhibited a different behavior. The emission maximum had a red shifting trend, from 514 to 544 nm as the size of the ordered clusters decreased (from **CPA1** to **CPA5**), in agreement with literature reports [56, 58, 62]. The quantum yield of the xerogels had values on a larger range, from 9.8 to 51 %, strongly related to exciting light energy. The highest values from 40.4 to 51 % were registered when excited with UV light of higher energy (360 nm), while the lowest values from 9.8 to 14.3 % where obtained when excited with the light of lower energy attributed to D→A intramolecular charge transfer (480 nm). Almost similar values for both hydrogels and xerogels were obtained when excited with UV light of energy corresponding to π-π* electron transition of the conjugated skeleton. The color of the light emitted by the xerogels laid in the gamut of the human vision in almost all cases, spanning from blue-green to yellowish-green (Figure 7d, e, f), as can be also seen when samples were illuminated with an UV lamp (Figure 7g-k).

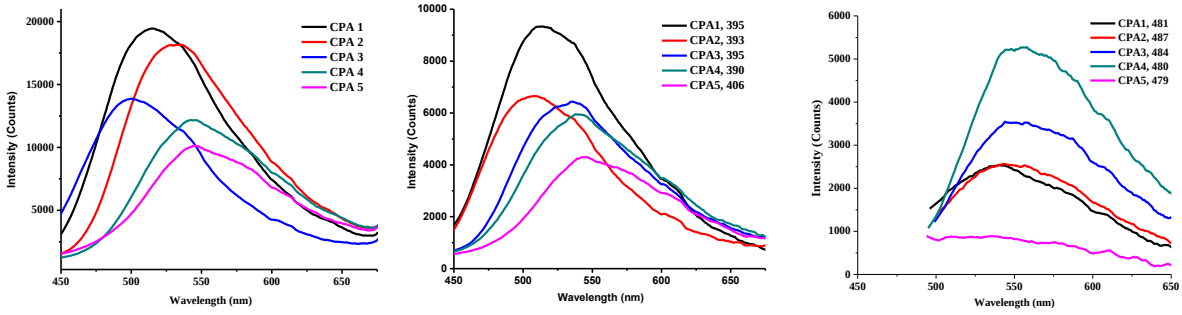

a) **b)** **c)**

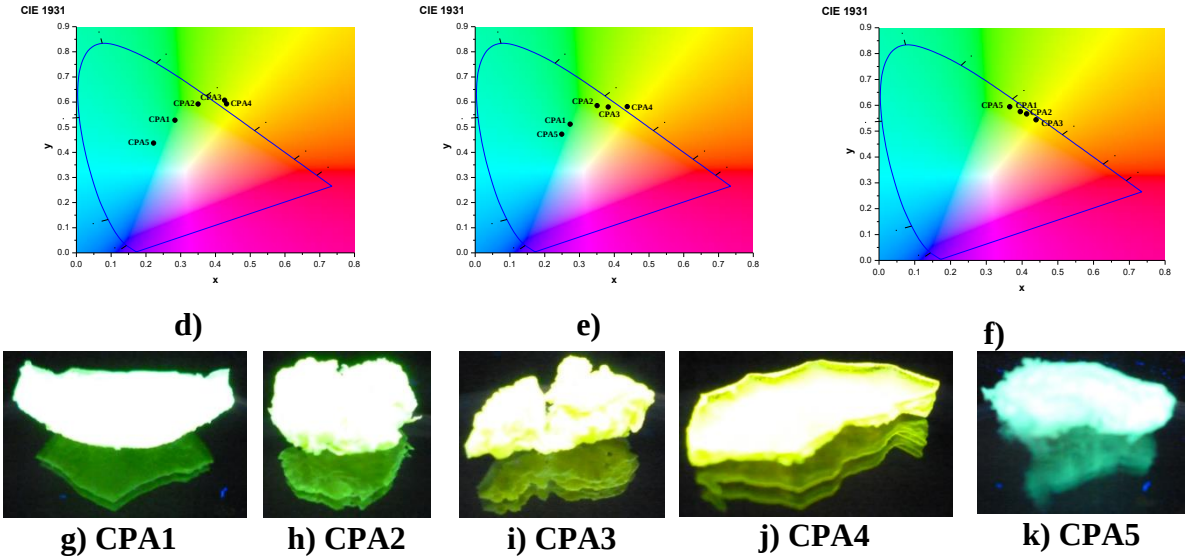

Figure 7. Emission spectra and corresponding chromaticity diagrams of xerogel samples excited with light of a), d) 360 nm, b), e) around 390 nm, c), f) around 395 nm (the exact wavelength is given in the inset of the graph) and g-h) images of the xerogels illuminated with an UV-lamp

The notable emission properties of the studied hydrogels and xerogels have been mainly attributed to the formation of phenothiazine based ordered clusters within the chitosan network which significantly improved the quantum efficiency due to the high surface-to-volume ratio aspect. The formation of some isolated phenothiazine-imine units on chitosan chains or some traces of unreacted aldehyde must have an important influence on the quantum yield improving, too. On the other hand, the immobilization of the ordered clusters within the chitosan network has to lower the diffusion quenching, favouring photoluminescence intensifying. The lower luminescence of the hydrogels as compared to xerogels could be ascribed to the presence of water which promotes luminescence quenching by a non-radiative process through O-H vibrations of the water molecules. An important factor in improving the quantum yield appears to be the porous morphology of the xerogels, probably by additional increasing of the surface-to-volume ratio aspect.

The luminescence of both hydrogels and xerogels was well preserved during the time. Measurements of the quantum yield over 3 months, on the same samples hold in laboratory conditions at room temperature, gave similar values with those measured on freshly prepared hydrogels and xerogels, proving the good photoluminescence stability of the samples, an important feature in optoelectronic applications.

Mechanical properties

An important advantage of organic materials *versus* the inorganic ones for optoelectronics application is their facile processability as thin films with good mechanical properties. A preliminary study of the processability and mechanical properties of the studied hydrogels shown that they were able to give thin, flexible films with good mechanical toughness under the pressure of an external stress as bending, elongation or even attaching of a balance weight; a film of 5 cm/1 cm/0.2 cm was able to sustain a balance weight of 5 g over one week, without breaking (Figure 8). When applying different elongation percent between 20 and 100 %, the hydrogels suffered a viscoelastic loss between 5 and 35 % (Figure 8a). Their breaking occurred at a high tensile strength of 0.22 MPa, at a strain of 92 % (Figure 8b).

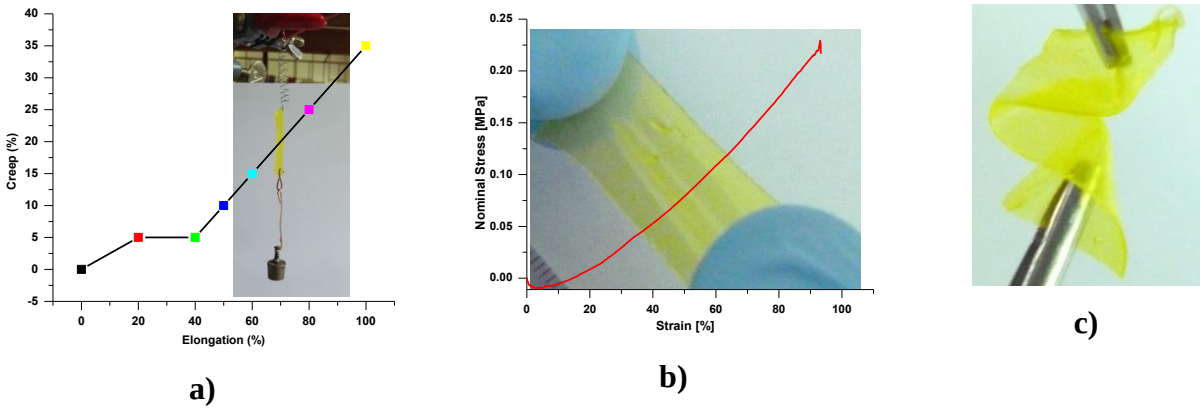

Figure 8. Mechanical properties of the representative **CPA1** hydrogel: a) creep-elongation curve with the image of hydrogel sustaining a balance weight; b) stress-strain curve with the image of the bended hydrogel under UV light

Conclusions

The paper brings into attention a new type of eco-friendly luminescent hydrogels prepared by acid condensation reaction of the amine groups of chitosan with aldehyde bearing phenothiazine. The hydrogelation take place due to the self-ordering of the chitosan segments grafted with rigid imine units, facilitated by the ability of carbonyl-amine/imine interconversion system, to afford ordered clusters acting as network nodes. The hydrogels have a microporous morphology with very thin pore walls and good mechanical toughness. The use of the phenothiazine aldehyde to crosslink the chitosan polyamine proved to be an excellent route toward highly luminescent stable materials – a quantum yield of 32.8 % was reached for the hydrogels and of 51% for the xerogels. The high quantum efficiency has been attributed to the synergistic influence of (i) the phenothiazine heteroaromatic ring (ii) formation of ordered

clusters with a high surface-to-volume ratio; (iii) microporous morphology which further enhances the active surface.

All these results demonstrate a new, original approach in exploiting chitosan biopolymer, paving the way towards efficient luminescent biomaterials.

Acknowledgements

The paper is part of a project financed through a Romanian National Authority for Scientific Research MEN – UEFISCDI grant, project number PN-II-RU-TE-2014-4-2314 and through the European Union's Horizon 2020 research and innovation programme under grant agreement 667387.

The authors are thankful to Professor Mihai Barboiu, Institut Européen des Membranes, Montpellier, France for useful discussions related to the reversibility of the imine linkage on chitosan.

References

[1] H. Sasabe, J. Kido, *J. Mater. Chem. C*., 2013, **1**, 1699-1707.

[2] Y. Hong, J. W. Y. Lam, B. Z. Tang, *Chem. Soc. Rev.*, 2011, **40**, 5361-5388.

[3] A.M. Schmidt, *Colloid Polym. Sci.*, 2007, **285**, 953-966.

[4] Z. Hu, T. Cai, C. Chi, *Soft Mater*, 2010, **6**, 2115-2123.

[5] C. Y. Chen, C. T. Chen, *Chem. Commun.*, 2011, **47**, 994-996.

[6] L. Wang, Z. Sun, M. Ye, Y. Shao, L. Fang, X. Liu, *Polym. Chem*., 2016, **7**, 3669-3673.

[7] M. O'Neill, S.M. Kelly, *Adv. Mater.*, 2003, **15**, 1135-1146.

[8] B. A. Gregg, M. A. Fox, A. J. Bard, *J. Phys. Chem.* 1990, **94**, 1586-1598.

[9] F. Camerel, L. Bonardi, G. Ulrich, L. Charbonnière, B. Donnio, C. Bourgogne, D. Guillon, P. Retailleau, R. Ziessel, *Chem. Mater.* 2006, **18**, 5009-5021.

[10] J. Y. R. Silva, L. L. da Luz, F. G. M. Mauricio, I. B. V. Alves, J. N. de Souza Ferro, E. Barreto, I. T. Weber, W. M. de Azevedo, S. A. Júnior, *ACS Appl. Mater. Interfaces* 2017, **9**, 16458-16465.

[11] P. Chawla, A. Ranjan Srivastava, P. Pandey, V. Chawla, *Mini-Rev. Med. Chem.* 2014, **14**, 154-167.

[12] M. L. Oyen, *Int. Mater. Rev.* 2014, **59**, 44-59.

[13] H. Bildirir, V. G. Gregoriou, A. Avgeropoulos, U. Scherf, C. L. Chochos, *Mater. Horiz.* 2017, **4**, 546-556.

[14] C. P. McCoy, *Chem. Mater.* 2006, **18**, 4336-4343.

[15] G. Liu, Y. M. Zhang, X. Xu, L. Zhang, Y. Liu, *Adv. Opt. Mater.* 2017, **5**, 1700149.
[16] Q. F. Li, X. Du, L. Jin, M. Hou, Z. Wang, J. Hao, *J. Mat. Chem. C*, 2016, **15**, 3195-3201.
[17] Y. Liu, T. Wang, M. Liu, *Chem. - Eur. J.*, 2012, **18**, 14650-14659.
[18] T. Friedrich, B. Tieke, *Colloid Polym. Sci.*, 2010, **288**, 1479-1484.
[19] A.J. Ragauskas, C. K. Williams, B. H. Davison, G. Britovsek, J. Cairney, C. A. Eckert, W. J. Frederick, J. P. Hallett, D. J. Leak, C. L. Liotta, *Science*, 2006, **311**, 484-489.
[20] A.Chang, J. Peng, L. Zhang, D. W. Pang, *J. Mater. Chem.*, 2009, **19**, 7771-7776.
[21] J. Huo, Y. Zheng, S. Pang, Q. Wang, *Cellulose*, 2013, **20**, 841-848.
[22] Z. Zhoub, Q. Wang, *Sens. Actuators, B.*, 2012, **173**, 833-838.
[23] H. Huang, W. Song, G. Chen, J. M. Reynard, T. Y. Ohulchanskyy, P. N. Prasad, F. V. Bright, J. F. Lovell, *Adv. Healthcare Mater.*, 2014, **3**, 891-896.
[24] F. F. da Silva, F. L. de Menezes, L. L. da Luz, S. Alves Jr., *New J. Chem.*, 2014, **3**, 893-896.
[25] X. Guo, C. F. Wang, Y. Fang, L. Chen, S. Chen, *J. Mater. Chem.*, 2011, **21**, 1124-1129.
[26] Y. Wu, L. Wang, Y. Qing, N. Yan, C. Tian, Y. Huang, *Sci. Rep.*, 2017, **7**, 4380.
[27] T. Fine, P. Leskinen, T. Isobe, H. Shiraishi, M. Morita, R.S. Marks, M. Virta, *Biosens. Bioelectron.*, 2006, **21**, 2263-2269.
[28] Q. Dong, W. Qu, P. Wang, W-Y. Wong, *Polym. Chem.*, 2016, **7**, 3827-3831.
[29] R. Shepherd, S. Reader, A. Falshaw, *Glycoconjugate J.*, 1997, **14**, 535-542.
[30] L. Marin, S. Morariu, M. C. Popescu, A. Nicolescu, C. Zgardan, B. C. Simionescu, M. Barboiu, *Chem. - Eur. J.*, 2014, **20**, 4814-4821.
[31] L. Marin, B. C. Simionescu, M. Barboiu, *Chem. Commun.*, 2012, **48**, 8778-8780.
[32] D. Ailincai, L. Marin, S. Morariu, M. Mares, A. C. Bostanaru, M. Pinteala, B. C. Simionescu, M. Barboiu, *Carbohydr. Polym.*, 2016, **152**, 306-316.
[33] M. Iftime, S. Morariu, L. Marin, *Carbohydr. Polym.*, 2017, **265**, 39-50.
[34] L. Marin, D. Ailincai, S. Morariu, L. Tartau-Mititelu, *Carbohydr. Polym.*, 2017, **170**, 60-71.
[35] A. M. Olaru, L. Marin, S. Morariu, G. Pricope, M. Pinteala, L. Tartau-Mititelu, *Carbohydr. Polym.* **2017**, doi.org/10.1016/j.carbpol.2017.09.066
[36] Shigehiro Hirano, Ryuji Yamaguchi, Noriaki Matsuda, Osamu Miura, Yotaro Kondo, Chitosan-aldehyde Gel A Novel Polysaccharide Gel Produced from Chitosan and Aldehydes, Agric . Biol. Chem., 1977, 41 (8), 1547-1548
[37] A. Bejan, S. Shova, M. D. Damaceanu, B. C. Simionescu, L. Marin, *Cryst. Growth Des.*, 2016, **16**, 3716-3730.

[38] A. Zabulica, M. Balan, S. Belei, M. Sava, B. C. Simionescu, L. Marin, *Dyes Pigm.*, 2013, **96**, 686-692.

[39] L. Marin, A. Bejan, D. Ailincai, D. Belei, *Eur. Polym. J.*, 2017, **95**, 127-137.

[40] D. Belei, C. Dumea, E. Bicu, L. Marin, *RSC Adv.*, 2015, **5**, 8849-8858.

[41] S. Kumar, J. Dutta, P. K. Dutta, J. Macromol. Sci. Pure, 2009, **46**, 1095-1102.

[42] J. E. dos Santos, E. R Dockal, E. T. G. Cavalheiro, *Carbohydr. Polym.*, 2005, **60**, 277-282.

[43] S. Destri, I. A. Khotina, W. Porzio, *Macromolecules*, 1998, **31**, 1079-1086.

[44] H. Wang, W. Xu, B. Zhang, *J. Chem. Cryst.* 2012, **42**, 846-850.

[45] T. Treeudom, S. P. Wanichwecharungruang, J. Seemork, S. Arayachukeat, *Carbohydr. Polym.*, 2011, **86**, 1602-1609.

[46] D. Ailincai, C. Farcau, E. Paslaru, L. Marin, *Liq. Cryst.*, 2016, **43**, 1973-1985.

[47] A. J. Lovinger, K. R. Amundson, D. D. Davis, *Chem Mater.*, 1994, **6**, 1726-1736.

[48] M. Baron, *Pure Appl. Chem.*, 2001, **73**, 845-895.

[49] A. G. Rusu, M. I. Popa, G. Lisa, L. Verestiuc, *Thermochim. Acta*, 2015, **613**, 28-40.

[50] P. Kovaricek, J. M. Lehn, *J. Am. Chem. Soc.*, 2012, **134**, 9446-9455.

[51] G. Nasr, E. Petit, D. Vullo, J. Y. Winum, C. T. Supuran, M. Barboiu, *J. Med. Chem.*, 2009, **52**, 4853-4859.

[52] A. Zabulica, E. Perju, M. Bruma, L. Marin, *Liq. Cryst.*, 2014, **41**, 252-262.

[53] J. S. Basuki, A. Jacquemin, L. Esser, Y. Li, C. Boyer, T. P. Davis, *Polym. Chem.*, 2014, **5**, 2611-2620.

[54] N. Egashira, K. Yamamoto, J. Kadokawa, *Polym Chem.*, 2017, **8**, 3279-3285.

[55] F. Laatar, M. Hassen, C. Amri, F. Laatar, A. Smida, H. Ezzaoui, *J. Lumin.*, 2016, **178**, 13-21.

[56] Y. Hong, J. W. Y. Lama, B. Z. Tang, *Chem. Commun.*, 2009, 0, 4332-4353.

[57] R. Yoshii, A. Hirose, K. Tanaka, Y. Chujo, *Chem. - Eur. J.*, 2014, **20**, 8320-8324.

[58] Y. S. Zhao, H. Fu, A. Peng, Y. Ma, D. Xiao, J. Yao, *Adv. Mater.*, **2008**, **20**, 2859-2876.

[59] E. Gal, L. Găină, C. Cristea, V. Munteanu, L. Silaghi-Dumitrescu, *J. Electroanal. Chem.*, 2015, 770, 14-22.

[60] E. Kwon, H. Oikawa, H. Kasai, H. Nakanishi, *Cryst. Growth Des.*, 2007, **7**, 600-602.

[61] Z. Iqbal, W. Q. Wu, D. B. Kuang, L. Wang, H. Meier, D. Cao, *Dyes Pigm.*, 2013, **96**, 722-731.

[60] L. Marin, S. Shova, C. Dumea, E. Bicu, D. Belei, *Cryst. Growth Des.*, 2017, **17**, 3731-3742.